



## Analysis of Tide Gauge Data at Baía de Paranaguá, PR

### *Análise de Dados Maregráficos na Baía de Paranaguá, PR*

Raimundo Sales de Melo Neto <sup>1</sup>, Cláudia Pereira Krueger <sup>2</sup> and Regiane Dalazoana <sup>3</sup>

<sup>1</sup> Federal University of Paraná, Curitiba, Brazil. [demeloneto@gmail.com](mailto:demeloneto@gmail.com)

ORCID: <https://orcid.org/0009-0004-3649-4337>

<sup>2</sup> Federal University of Paraná, Curitiba, Brazil. [ckrueger@ufpr.br](mailto:ckrueger@ufpr.br)

ORCID: <https://orcid.org/0000-0002-4839-1317>

<sup>3</sup> Federal University of Paraná, Curitiba, Brazil. [regiane@ufpr.br](mailto:regiane@ufpr.br)

ORCID: <https://orcid.org/0000-0001-5468-0679>

Received: 12.2025 | Accepted: 01.2026

**Abstract:** This study analyzes tide gauge data from Paranaguá Bay, in Paraná, Brazil, aiming at characterizing tidal patterns using time series analysis. The methodology comprised the development and application of quality control procedures aiming at identifying and removing spurious data. These procedures resulted in a 9.86% reduction in the variance of harmonic constituents, enabling a substantially larger number of constituents to be resolved across several time series. Harmonic analysis was performed using the AstGeoTop and PACMARÉ software packages. Predominantly semidiurnal tidal behavior was identified at stations located in the middle and inner portions of the bay, whereas a semidiurnal regime with pronounced inequalities prevailed near the bay entrance. Based on the Reduction in Variance (RV) index, harmonic reconstruction accounted, on average, for 82% of observed sea level variability, indicating an approximate 18% contribution from meteorological forcing within the study area. The application of Thompson's low-pass filter allowed the seasonal structure of tidal residuals to be delineated, revealing positive sea level anomalies during the first half of the year and negative anomalies during the second half. Although the available time series are not sufficiently long to support robust long-term assessments, the results underscore the importance of maintaining continuous tide gauge records for coastal research. Furthermore, the lack of complementary meteorological data constrained a fully integrated analysis of atmospheric forcing and its influence on regional sea level variability.

**Keywords:** Harmonic analysis. Quality control. Vertical datum. Time series.

**Resumo:** Este estudo analisa dados maregráficos da Baía de Paranaguá, no Paraná, visando compreender os padrões de maré por meio de séries temporais. A análise incluiu o desenvolvimento e aplicação de processos para remoção de dados espúrios. Esses processos foram capazes de reduzir a variância das constituintes resolvidas pela análise harmônica em 9,86%, permitindo a identificação de número significativamente maior de constituintes em diversas séries. A análise harmônica foi realizada pelos programas AstGeoTop e PACMARÉ. Observou-se comportamento predominantemente semidiurno nas estações maregráficas localizadas na parte média e interior da baía, e padrão semidiurno com desigualdades nas estações próximas à desembocadura. Utilizando o índice RV, pode-se concluir que a maré reconstituída pela análise harmônica explicou, em média, 82% da variação da maré nos períodos analisados, ou seja, uma influência de maré meteorológica de, aproximadamente, 18% na área de estudo. A utilização do filtro passa-baixa de Thompson possibilitou delinear a predominância da maré ao longo do ano a partir dos resíduos, com marés positivas no primeiro semestre e negativas no segundo. Embora as séries temporais não apresentem duração suficiente para análises de longo prazo, este estudo reforça a importância da manutenção de registros maregráficos para subsidiar estudos nas zonas costeiras. Adicionalmente, a ausência de dados meteorológicos complementares limitou a capacidade de análise integrada das forçantes atmosféricas e sua influência sobre o nível do mar na região.

**Palavras-chave:** Análise Harmônica. Controle de Qualidade. Referencial Vertical. Séries Temporais.

## 1 INTRODUCTION

Brazil has an extensive coastal zone characterized by diverse oceanographic and climatic conditions, a wide variety of coastal morphologies, ecosystems, and socio-economic activities, forming highly biodiverse coastal systems (Moura Neto & Azevedo, 2022). This maritime domain is encompassed by the concept of the Blue Amazon, which refers to the oceanic area under Brazilian jurisdiction, including territorial waters, the seabed, and subsoil, and is recognized as strategic for national development, environmental protection, scientific research, and sovereignty (Marinha do Brasil, 2025b). Within this framework, the coastal zone constitutes a cornerstone of the blue economy, integrating port infrastructure, logistical chains, and maritime routes that are essential for Brazil's participation in international trade (Andrade et al., 2024).

Paranaguá Bay exemplifies this strategic setting. The Port of Paranaguá stands out as a major logistics hub and recorded successive cargo records in 2025 (Governo do Estado do Paraná, 2025a; 2025b). This growing relevance reinforces the need to understand the role of meteorological tides, as associated sea level variability may directly affect vessel maneuverability and the operational safety of port facilities. International evidence indicates that high-tide flooding events are likely to become more frequent under scenarios of relative sea level rise, increasingly demanding large-scale engineering interventions to mitigate impacts on coastal infrastructure (Sweet et al., 2018). Therefore, neglecting the meteorological contribution to sea level variability entails significant economic, social, and environmental risks.

In the context of coastal and port engineering, accurate knowledge of seasonal tidal oscillations and residual sea level variability is essential for planning dredging operations and berthing activities, contributing to cost reduction and enhanced operational safety. In Paranaguá, for instance, a 30 cm increase in draft has resulted in an approximate 2,000-ton increase in the loading capacity of bulk carriers (Governo do Estado do Paraná, 2025c). From a coastal risk management perspective, characterizing seasonal patterns and extreme events associated with meteorological tides supports the development of early warning systems, such as those implemented along the São Paulo coastline (Secretaria do Meio Ambiente, Infraestrutura e Logística, 2024). Over longer timescales, the maintenance of continuous tide gauge records enables the detection of local sea level rise trends and their relationship with increasing coastal flooding frequency, providing direct input for coastal and port adaptation planning (Sweet et al., 2018).

This context intensifies the growing demand for cartographic products at multiple spatial scales, which are fundamental for environmental risk management, navigational safety, and coastal engineering design. Altimetric and hydrographic surveys play a central role in this process by providing the foundation for the definition of consistent vertical reference systems.

Precise definition of vertical reference levels is essential in both nautical and terrestrial cartography. In hydrographic applications, charted depths must be referenced to the tidal regime, making the analysis of tide gauge time series a critical component in defining vertical reference surfaces. In contrast, physically based height systems are referenced to an equipotential surface of the Earth's gravity field, such as the geoid.

The discrepancy between Mean Sea Level (MSL) and the geoid became evident in the 1980s with advances in satellite altimetry (ALTSAT), leading to the concept of Mean Sea Level Topography (MSLT) (Silva & Freitas, 2019). Despite its transformative impact on geodetic and oceanographic research, satellite altimetry exhibits notable limitations in coastal environments due to sea surface roughness and signal contamination from adjacent land topography (Dalazoana, 2006).

In this setting, tide gauges remain indispensable for monitoring sea level variability. Modern instruments operate at high sampling rates, enabling continuous and near-real-time measurements, thereby expanding their applicability to extreme event analysis, storm surge forecasting, and navigational safety. Historical paper-based records have largely been replaced by digital measurements with sampling intervals as short as one second.

Nevertheless, tide gauge records are subject to multiple sources of error that may compromise data homogeneity and reliability. According to Hague et al. (2022), these include station relocation, vertical datum changes, modifications in data processing procedures, equipment replacement, and data gaps arising from operational or transmission failures. Ensuring the consistency and reliability of tide gauge records

therefore requires systematic identification and correction of such anomalies, as well as the provision of transparent data quality indicators to end users.

Given this scenario, this study analyzes tide gauge data from Paranaguá Bay, Paraná State, with particular emphasis on quality control procedures and data processing techniques, including harmonic analysis, low-pass filtering, and statistical methods. The effectiveness of these approaches in minimizing inconsistencies and improving the accuracy of vertical references derived from time series is assessed, providing technical support for applications in navigational safety, coastal engineering, and geodetic research.

## 2 METHODOLOGY

### 2.1 Study Area

Paranaguá Bay is located within the Paranaguá Estuarine Complex (PEC), one of the most important estuarine systems along the southern coast of Brazil. Situated in the central-northern portion of the Paraná coastline, the PEC is characterized by a complex network of interconnected channels and bays. This estuarine system is composed of two main branches: one oriented in an east–west direction, approximately 50 km in length, encompassing Paranaguá and Antonina bays, where the Port of Paranaguá, one of the busiest ports in Brazil, is located; and a second branch oriented in a north–south direction, comprising Laranjeiras Bay, the Guaraqueçaba sub-estuary, and the Internal Access Channel to Pinheiros Bay (Marone et al., 2007). Regional hydrodynamics are strongly influenced by the tidal regime, making the use of reliable tide gauge time series essential for understanding oceanographic processes that affect vertical reference surfaces.

### 2.2 Tide Gauge Data

A total of 38 time series from six tide gauge stations (TGS) located in Paranaguá and Antonina bays were analyzed. The data were collected using float-and-counterweight, pressure, and radar sensors, with acquisition intervals ranging from five minutes to one hour. All datasets were obtained from the National Oceanographic Data Bank (NODB), a service operated by the Brazilian Navy Hydrographic Center (BNHC). The tide gauge stations used in this study are listed in Table 1 and are identified by the trigram shown in parentheses following each station name

Table 1 – Tide gauge stations analyzed and general characteristics of the time series.

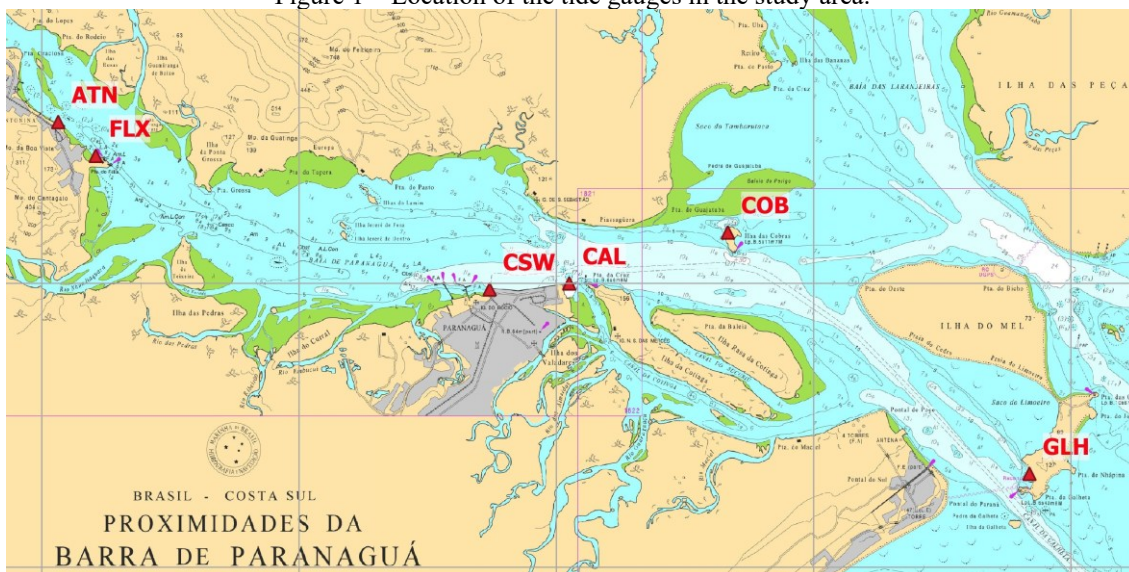
Station Name	Number of time series	Sensor Type	Observation period	Duration in days
Antonina (ATN)	2	Float and Counterweight	1995 - 1997	413
Ilha das Cobras (COB)	3	Float and Counterweight, RADAR	1975 - 2018	152
Cais Oeste (CSW)	15	Float and Counterweight, Pressure Sensor	1992 - 2019	3259
Galheta (GLH)	12	Float and Counterweight, Pressure Sensor	1975 - 2019	2268
Ponta do Felix (FLX)	5	Float and Counterweight	2000 - 2002	629
Cais Leste (CAL)	1	RADAR	2016	109

Source: The authors (2025).

The NODB also provides the Tide Gauge Station Description Sheets (F-41), a document in which the Brazilian Navy Hydrographic Center (BNHC) records the information required to reconstruct a given tide gauge station, when necessary, in support of Hydrographic Surveys (HS). This document includes: the geographic location of the tide gauge station and all leveling benchmarks (BM) used during its installation; the observation period adopted for the computation of the local mean sea level and the chart datum (CD); the height differences between the benchmarks and the staff gauge used during the observation period; the length of the staff gauge corresponding to the observation interval; among other information deemed relevant (Brazilian Navy, 2023). The chart datum (CD) is the vertical reference for depths depicted on nautical charts produced by the BNHC and is equivalent to the mean low water springs.

Figure 1 illustrates the spatial distribution of the tide gauges within the study area, overlaid on an excerpt of Nautical Chart No. 1820, obtained from the Brazilian Navy (2025a).

Figure 1 – Location of the tide gauges in the study area.



Source: Adapted from Brazilian Navy (2025a).

In addition to the data from Paranaguá Bay, this study also incorporated daily mean sea level records from the Cananéia tide gauge station (São Paulo State), obtained from the database of the University of Hawaii Sea Level Center (UHSLC) (Caldwell et al., 2015). The Cananéia station is located approximately 80 km from Paranaguá Bay and provides continuous records dating back to 1954, thereby contributing to the regional-scale analysis. Although cross-validation procedures (buddy checking) were not applied, this approach is widely recognized as an important tool in tide gauge data processing for identifying inconsistencies, instrumental drift, and datum shifts. Table 2 presents the main metadata for a representative subset of these time series, which are coded using the respective tide gauge station trigram followed by a letter, facilitating the distinction among different series from the same station.

Table 2 – Metadata of the most representative time series used in the study.

Station name	Series code	Sensor type	Sampling rate	Observation period	Duration in days
Antonina	ATN_B	Float and Counterweight	1 hour	01/01/1997 - 31/12/1997	365
Ilha das Cobras	COB_B	Float and Counterweight	1 hour	04/05/1995 - 21/06/1995	49
	COB_C	RADAR	5 minutes	31/05/2018 - 09/08/2018	71
Cais Oeste	CSW_B	Float and Counterweight	1 hour	02/01/1994 - 31/10/1994	303
	CSW_F	Float and Counterweight	1 hour	01/01/1997 - 31/12/1999	1095
	CSW_I	Float and Counterweight	1 hour	01/07/2001 - 27/10/2001	119
	CSW_J	Float and Counterweight	1 hour	29/10/2001 - 30/11/2002	398
	CSW_K	Float and Counterweight	1 hour	01/01/2003 - 31/12/2003	365
	CSW_L	Float and Counterweight	1 hour	02/01/2004 - 12/02/2004	42
	CSW_M	Float and Counterweight	1 hour	27/02/2004 - 31/12/2004	309
	CSW_N	Pressure	5 minutes	21/09/2018 - 14/03/2019	175
	CSW_O	Pressure	10 minutes	24/08/2018 - 19/11/2018	88
Galheta	GLH_B	Float and Counterweight	1 hour	26/04/1995 - 26/11/1995	215
	GLH_D	Float and Counterweight	1 hour	05/01/1996 - 18/01/1996	14
	GLH_E	Float and Counterweight	1 hour	01/05/1996 - 31/05/1996	31
	GLH_G	Float and Counterweight	1 hour	01/01/1997 - 31/12/1997	365
	GLH_J	Float and Counterweight	1 hour	09/05/2001 - 28/02/2005	1392
	GLH_K	Pressure	5 minutes	28/10/2018 - 29/11/2018	33
	GLH_L	Pressure	10 minutes	03/04/2019 - 20/05/2019	48
	Ponta do Felix	FLX_D	Float and Counterweight	1 hour	01/03/2001 - 03/05/2001
FLX_E		Float and Counterweight	1 hour	02/06/2001 - 21/06/2002	385
Cais Leste	CAL_0	RADAR	5 minutes	04/02/2016 - 22/05/2016	109

Source: The authors (2025).

## 2.3 Software

The processing of the time series involved the execution of quality control routines, harmonic analysis, mean sea level computation, filtering, and graphical visualization, requiring tools capable of handling long time series and providing flexibility throughout the analysis and post-processing stages.

Harmonic analysis was performed using the PACMARÉ and AstGeoTop software packages, selected for their robustness and widespread acceptance within the scientific community. PACMARÉ performs frequency-domain analyses and is employed by the Brazilian Navy Hydrographic Center (BNHC) for tidal prediction and the computation of daily mean sea level (Franco, 2009). In this study, the ANALEXEC module was applied through the ANHAMA interface, with constituent selection based on statistical significance criteria. Tidal constituents were rejected at a 95% confidence level, as described by Franco (2009).

For the processing of tide gauge data in AstGeoTop, the “Tide Analysis” module was employed (Garnés, 2021). This module applies time-domain analysis methods and complemented the quality control performed with PACMARÉ, as it is particularly effective for the analysis of time series containing data gaps.

Quality control, resampling, filtering, and data editing routines were implemented in Python, using libraries such as NumPy (Harris et al., 2020), Matplotlib (Hunter, 2007), and SciPy (Virtanen et al., 2020). The R programming language (R Core Team, 2022) was used for complementary statistical analyses, while electronic spreadsheets and geographic information systems (GIS) were employed for data organization and visualization. The combined use of these tools provided flexibility in time series manipulation and ensured methodological rigor throughout the quality control process.

## 2.4 Quality Control

Quality control constitutes a critical stage in tide gauge data processing, as errors arising from instrumental, human, or environmental sources may introduce significant distortions into time series and directly compromise harmonic analysis. Accordingly, the systematic application of quality control techniques is essential to ensure data integrity, continuity, and representativeness.

The procedures adopted in this study aimed at: verifying potential changes in the vertical reference of tide gauge stations through the analysis of the F-41; identifying and removing spurious data; assessing time series quality; and preparing the datasets for subsequent processing.

To identify and remove spurious observations, tests and algorithms recommended under Level 2 (L2) mode described in Quality control of in situ sea level observations: A review and progress towards automated quality control (Vol. 1) (Intergovernmental Oceanographic Commission, 2020) were applied. This publication compiles standards and best practices for tide gauge data quality control. The L2 mode was adopted because the analyzed series are of sufficient duration to support the generation of derived products such as residuals, mean sea levels, extremes, and harmonic constants, which is consistent with the objectives of this study.

The Intergovernmental Oceanographic Commission (2020) coordinates global sea level observation initiatives, such as the Global Sea Level Observing System (GLOSS), which promotes the deployment of high-quality tide gauge networks for climate, oceanographic, and coastal research, fostering standardized approaches to tide gauge data quality control.

The quality control procedures were automated using Python scripts organized into two phases. In the first phase, operations were applied directly to the original time series to identify and remove spurious data. Subsequently, harmonic analysis was performed on the filtered series, and a reconstructed series (astronomical tide) was generated. Subtracting the reconstructed series from the original data yielded the residual series, which then became the focus of the second phase, in which gross errors are more readily detectable. Outlier detection applied to the residual series enabled further refinement of the quality control process.

The following steps were performed during the first phase:

- a) Verification of date and time record integrity: The algorithm scanned the time series to identify temporal gaps. When gaps were detected, they were filled with NaN (Not a Number) values, preserving the temporal structure of the series for subsequent processing;
- b) Approximation of the tide gauge series using sectionally continuous quadratic polynomials (second-degree splines) with 16 knots: The Least Squares Univariate Spline (LSQUnivariateSpline) technique, implemented via the SciPy library in Python (Virtanen et al., 2020), was applied. This method fits quadratic splines to valid observations by minimizing the sum of squared residuals between observed values and the fitted curve. Spline knots were defined every 16 observations. The resulting spline,  $S(t)$ , represents the smoothed trend of the series, and residuals  $R(t)$  were computed as  $R(t) = X(t) - S(t)$ , in which  $X(t)$  denotes the tide gauge series. Observations whose absolute residuals exceeded three times the standard deviation of the residual series were classified as spurious and replaced with NaN values;
- c) Analysis of the rate of water level change, adopting a threshold of  $1 \text{ m h}^{-1}$ : The algorithm computed the absolute difference between consecutive observations. Whenever this difference exceeded the maximum threshold established according to the sampling interval, the observation was classified as spurious, provided that the preceding observation had not been previously flagged. Flagged values were subsequently replaced with NaN. The adopted thresholds were 100 cm for hourly series, 35 cm for 10-minute series, and 30 cm for 5-minute series. The reference value was defined based on the relationship between discharge and water level variation proposed by Marone et al. (2007) and an estimated maximum discharge of  $20,000 \text{ m}^3 \text{ s}^{-1}$  for the Galheta Channel (Amb Planejamento Ambiental e Biotecnologia Ltda, 2005), which would result in a rate of approximately  $0.49 \text{ m h}^{-1}$ . To ensure a conservative margin, this value was increased by 100%;
- d) Stability test with NaN replacement for prolonged sequences of constant values: The algorithm identified stationary segments potentially associated with instrumental malfunction. When the number of repeated values exceeded thresholds defined according to the sampling interval, all values in the segment were classified as spurious and replaced with NaN. The adopted thresholds were six observations for hourly series, eighteen for 10-minute series, and thirty-six for 5-minute series. These thresholds were conservatively defined to avoid the inadvertent removal of genuine tidal plateaus (slack water);
- e) Verification of anomalous amplitudes: Observations whose absolute difference relative to the series mean exceeded 2.74 m were classified as spurious and replaced with NaN. This threshold corresponds to the total tidal range reported by Camargo and Harari (2003), with an additional 100% safety margin to reduce the risk of excluding legitimate water level variations.

In the second phase, the filtered series from the first stage was subjected to harmonic analysis using AstGeoTop, which is suitable for series containing NaN values. The reconstructed series (astronomical tide), subtracted from the original observations, yielded the residual series, which was again analyzed using quadratic splines to refine outlier detection. Observations whose residuals exceeded the threshold ( $>3\sigma$ ) were replaced with NaN values. The treatment of NaN values varied according to the specific case: isolated values were filled using the mean of neighboring observations, whereas extended gaps followed the procedure recommended by Intergovernmental Oceanographic Commission (2020), namely linear interpolation of residuals combined with the addition of the predicted tide obtained from harmonic analysis.

Finally, the resulting time series were resampled to hourly intervals using filters described by Pugh (1987), with the objective of standardizing the datasets for subsequent processing stages. The series were then formatted according to the input requirements of the PACMARÉ system. This procedure aimed to maximize the reliability of the time series and to enhance the accuracy of the tidal constituents derived from harmonic analysis. The adopted methodology reinforces the robustness of the results and may serve as a methodological basis for future applications involving tide gauge time series.

A summary table presenting the main quality control tests and criteria adopted in this study is provided below.

Chart 1 – Summary of the tests and criteria applied in the quality control process.

Procedure	Description
Date and time verification	Identification of gaps in the temporal sequence of the series; missing records are replaced with NaN to preserve the chronological integrity of the data.
Tidal time series spline analysis	Application of the LSQUnivariateSpline technique (degree 2, 16 knots); observations with residuals exceeding $3\sigma$ were classified as spurious and replaced with NaN.
Water level rate-of-change analysis	Observations showing variations greater than 100 cm/h (1 h), 35 cm (10 min), or 30 cm (5 min) relative to the previous record were considered spurious and replaced with NaN.
Stability test	Detection of sequences of constant values with 6 (hourly), 18 (10 min), or 36 (5 min) consecutive observations; such segments were classified as spurious and replaced with NaN.
Amplitude verification	Observations whose deviation from the series mean exceeded 2.74 m were removed.
Residual series spline analysis	Application of the LSQUnivariateSpline technique to the residual series; observations whose residuals deviated by more than $3\sigma$ from the fitted spline were replaced with NaN.

Source: The authors (2025).

## 2.5 Data Processing

The processing of tide gauge data followed a structured workflow designed to extract relevant information: harmonic analysis; reconstruction of the series using the derived constituents; computation of residuals; application of filters to remove tidal signals; construction of histograms and spectral analyses to identify oscillations not explained by tidal constituents; statistical analysis of subtidal residuals; and calculation of monthly mean sea level.

The extraction of subtidal frequencies, associated with long-period oscillations linked to large-scale meteorological forcing (Melo Filho, 2017), was carried out through the application of a low-pass filter. Among the classical filters used in oceanography (Kalil, 1999), the Thompson filter was adopted due to its superior attenuation response near the cutoff frequency. The 120 weights applied in this study were computed by Oliveira (2004) specifically for Paranaguá Bay, taking into account the main local astronomical components as well as the inertial, or Coriolis, component ( $f = 2\Omega \sin \varphi$ , in which  $\Omega$  is the Earth's angular rotation rate and  $\varphi$  is the local latitude). The adopted cutoff frequencies were  $\Omega_1 = 6.4^\circ \text{ h}^{-1}$  and  $\Omega_2 = 11.2^\circ \text{ h}^{-1}$ , with the number of weights set to  $N = 120$ .

Distinguishing these tidal and subtidal frequency bands was fundamental for discriminating between tidal and meteorological components. Analysis of the subtidal components enabled the identification of the impact of meteorological phenomena on sea level oscillations in Paranaguá Bay and provided support for future research focused on the prediction of extreme events and the calibration of coastal hydrodynamic models.

## 3 RESULTS

### 3.1 Quality Control

The analysis of the F-41 revealed relevant inconsistencies in the information associated with the selected stations. For the Ilha das Cobras station, description sheets from different years exhibited inconsistencies between RN-1 and RN-2, indicating a probable recording error. At the Antonina station, unexpected variations were identified in the height differences between mean sea level (MSL) and benchmark RN-4, even after the declared relocation of the staff gauge. In addition, the absence of older description sheets for the Cais Oeste and Galheta stations prevented full temporal integration of their respective time series.

Following the documentary analysis, the quality control procedures described in Section 2.4 were applied to detect and correct spurious data. Among the 37 analyzed series, 25 (67.6%) exhibited removal rates below 0.5% of the total number of observations, indicating generally good data quality. In eight series (21.6%), removal rates ranged between 0.5% and 1.0%, and only four series (10.8%) showed removal rates exceeding 1%. The highest value occurred in the FLX\_D series, in which 2.02% of the records were replaced, a proportion still considered low with respect to preserving the overall integrity of the series. Table

3 presents the variance values of the tidal constituents and the number of constituents resolved by PACMARÉ for selected series, before and after filter application.

Across the full dataset, an average reduction of 9.86% in constituent variance was observed, indicating the effectiveness of the filtering procedure in noise removal. When analyzed by frequency band, the observed reductions were 10.38% for constituents with one cycle per day, 9.39% for two cycles per day, 8.86% for three cycles per day, and 10.81% for constituents with four cycles per day.

Among the most pronounced results, the CSW\_M series, with a duration of 309 days, exhibited variance reductions of 71% for one-cycle-per-day constituents and 57% for two-cycle-per-day constituents. Similarly, the GLH\_B series, spanning 215 days, showed reductions of 72% and 32%, respectively. In twelve series, the reduction in variance was accompanied by an increase in the number of resolved constituents, indicating enhanced spectral resolution and improved identification of tidal components.

Table 3 – Variance of tidal species and number of constituents determined for the filtered and original series.

Series	Variance of 1 cycle per day tidal species		Variance of 2 cycles per day tidal species		Number of determined constituents	
	Original	Filtered	Original	Filtered	Original	Filtered
COB_B	24,15	9,16	30,72	17,49	18	27
CSW_I	10,82	6,60	6,98	4,15	35	42
CSW_J	2,88	2,35	15,91	9,26	80	87
CSW_K	3,32	2,58	8,39	5,57	82	85
CSW_L	4,13	3,16	19,44	18,72	18	18
CSW_M	28,86	8,25	58,95	25,44	32	67
GLH_B	12,72	3,52	49,46	33,41	27	43
GLH_D	45,01	37,22	45,01	37,22	17	17
GLH_E	2,00	1,46	1,96	1,69	24	25
GLH_G	2,14	1,79	2,96	2,53	75	78

Source: The authors (2025).

The analysis of the F-41, combined with the application of the developed filter, resulted in rigorous quality control, enabling the selective removal of inconsistencies without compromising the representativeness of the time series. The results demonstrate that the adopted procedure enhanced data robustness and improved the identification of harmonic constituents, thereby ensuring the reliability of subsequent analytical stages.

## 3.2 Data Processing

### 3.2.1 HARMONIC ANALYSIS

Table 4 presents the results of the harmonic analysis for the longest filtered series from each tide gauge station: Antonina, Cais Oeste, and Galheta. For each series, the ten constituents with the largest amplitudes are shown for representational purposes, together with their respective standard deviations ( $\sigma$ ) of amplitudes and phases. Phase lags are referenced to the Greenwich meridian.

The results presented in Table 4 indicate that the M3 and M4 constituents exhibit amplitudes greater than those of the diurnal constituents, highlighting their influence on the tidal regime in Paranaguá Bay, in agreement with previous studies (Oliveira, 2004; Franz et al., 2016). Based on these constituents, the tidal type was determined according to the criterion proposed by Courtier (1938), as expressed in Eq. (1):

$$C = \frac{H(O1) + H(K1)}{H(M2) + H(S2)} \quad (1)$$

where,  $O1$ ,  $K1$ ,  $M2$  and  $S2$  are the principal diurnal and semidiurnal constituents, and  $H(i)$  denotes the amplitude of the  $i$ -th constituent. According to this criterion, when  $0 < C < 0.25$  the tide is classified as semidiurnal; when  $0.25 < C < 1.5$  it is classified as semidiurnal with diurnal inequality; when  $1.5 < C < 3.0$  it is classified as mixed; and when  $C > 3.0$  the tide is classified as diurnal.

Figure 2 presents the  $C$  values computed for the analyzed series, arranged from left to right in the

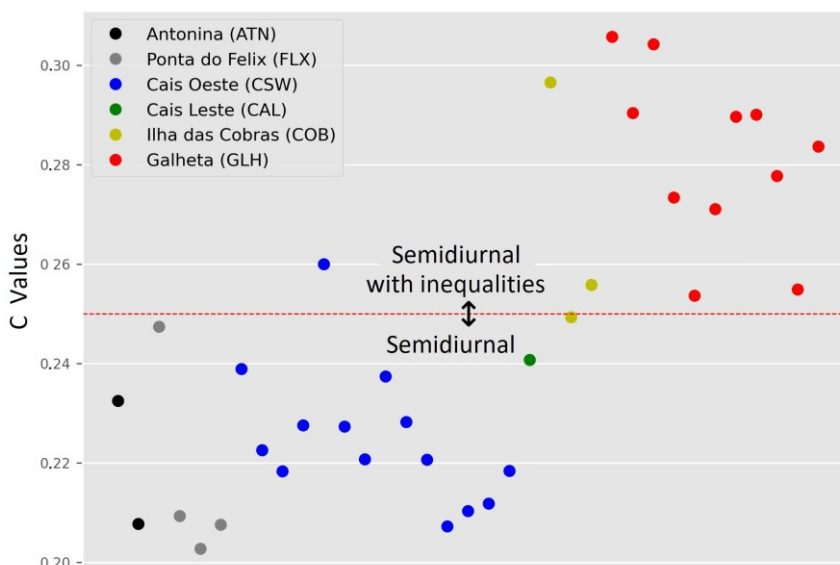
graph from Antonina to Galheta. The distribution of these values indicates a predominance of semidiurnal tides throughout the estuary, with more pronounced inequalities observed in the Galheta region, in agreement with the findings of Marone et al. (2013). Progressing toward the estuarine head, tidal characteristics become increasingly semidiurnal, reflecting the modification of the tidal regime along the estuarine gradient.

Table 4 – Amplitudes and phases of the constituents of the filtered series.

Series name	Constituent	Amplitude (cm)	Standard deviation of amplitude $\sigma_A$ (cm)	Fase (°)	Standard deviation of phase $\sigma_F$ (°)	
ATN_B	M2	53,48	0,53	196,69	0,55	
	S2	35,2	0,53	205,89	0,87	
	M4	25,43	0,78	122,54	1,64	
	M3	20,31	1,03	48,22	2,75	
	MS4	11,82	0,78	224,3	3,66	
	K2	11,09	0,53	197	3,68	
	O1	10,78	0,53	126,66	3,49	
	MN4	10,08	0,79	63,02	4,19	
	MO3	9,15	1,03	179,8	7,76	
	N2	8,74	0,54	263,83	3,41	
CSW_F	M2	48,3	0,26	186,98	0,30	
	S2	32,21	0,26	193,41	0,47	
	M4	16,06	0,31	89,22	1,05	
	M3	14,92	0,51	26,08	1,88	
	O1	11,19	0,24	124,56	1,51	
	K2	10,38	0,26	184,15	1,88	
	N2	7,8	0,26	124,56	1,51	
	K1	7,11	0,24	189,29	2,19	
	MO3	5,11	0,51	151,25	6,76	
	MS4	6,9	0,31	249,07	1,87	
	GLH_J	M2	36,88	0,23	71,19	0,36
		S2	24,41	0,23	177,89	0,54
O1		10,78	0,18	120,98	0,86	
K2		7,67	0,23	166,88	1,49	
M3		7,63	0,3	6,56	2,29	
M4		7,23	0,14	353,39	1,14	
K1		6,24	0,18	184,83	1,55	
N2		5,99	0,23	241,38	2,24	
MO3		4,12	0,3	183,49	3,83	
MK3		3,45	0,3	254,24	4,72	

Source: The authors (2025).

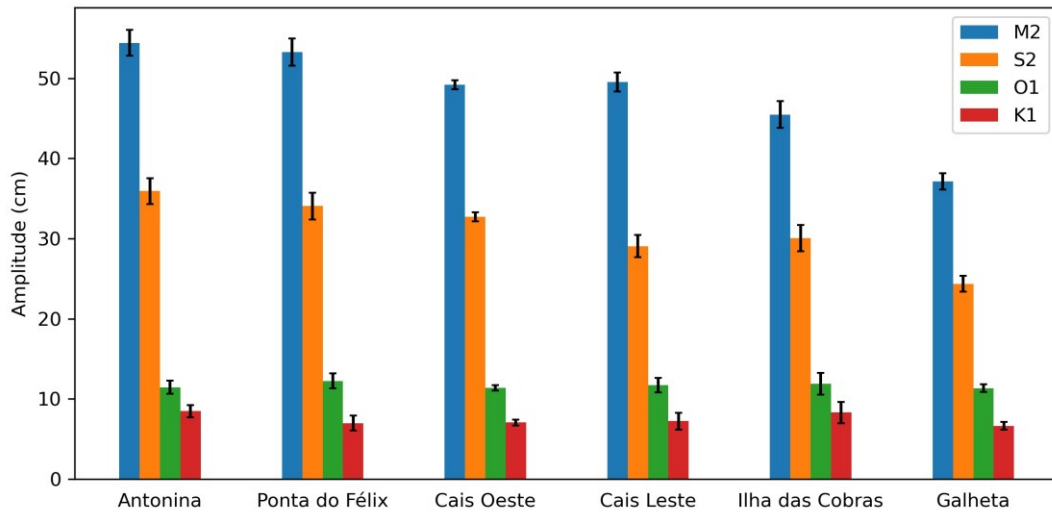
Figure 2 – Courtier criterion (C) derived from the individual series.



Source: The authors (2025).

Figure 3 presents the mean amplitudes of the constituents used in Eq. (1) for each tide gauge station. From Antonina toward Galheta, the semidiurnal constituents M2 and S2 exhibit a proportionally greater decrease than the principal diurnal constituents (O1 and K1), thereby accounting for the observed shift in tidal type.

Figure 3 – Amplitudes of the main diurnal and semidiurnal constituents.



Source: The authors (2025).

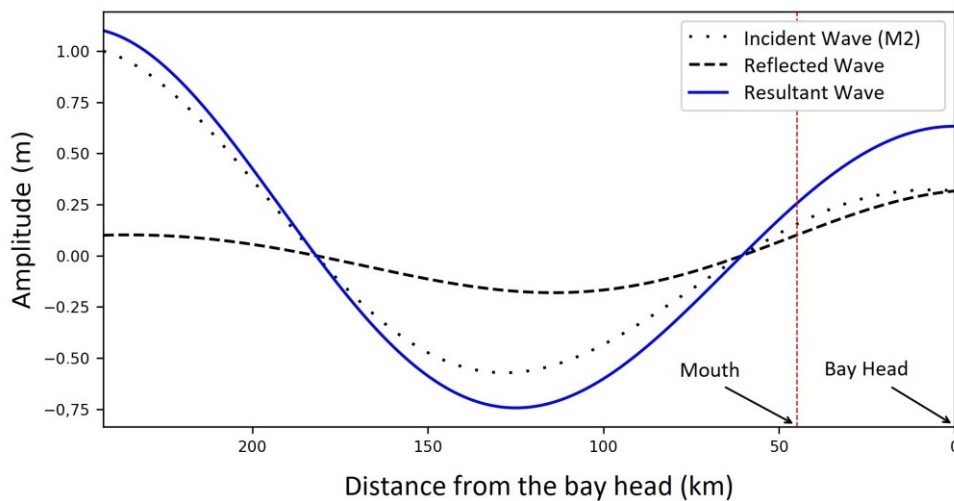
To assess the ability of the harmonic constants to reconstruct the tidal signal, the Reduction in Variance (RV) index was employed (Boon, 2007). This index corresponds to the ratio between the variance of the reconstructed tide and the variance of the observed tide, as expressed in Eq. (2):

$$RV = \frac{\sum [h(t) - h_0]^2}{\sum [h_t - h_0]^2} \tag{2}$$

where,  $h(t)$  represents the reconstructed tidal height at time  $t$ ;  $h_t$  denotes the observed tidal height at time  $t$ ; and  $h_0$  corresponds to the arithmetic mean of the observed tidal heights  $h_t$ . Based on the RV values obtained for all analyzed series, a mean RV of 0.82 was derived, indicating that approximately 18% of sea level variability can be attributed to meteorological tides.

In order to provide a basic understanding of the effect of reflection of the M2 constituent along Paranaguá Bay, a schematic propagation plot was constructed (Figure 4) using approximate parameters representative of the study area. This plot was based on the example presented by Boon (2007, p. 77).

Figura 4 – M2 amplitude in Paranaguá Bay.



Source: The authors (2025).

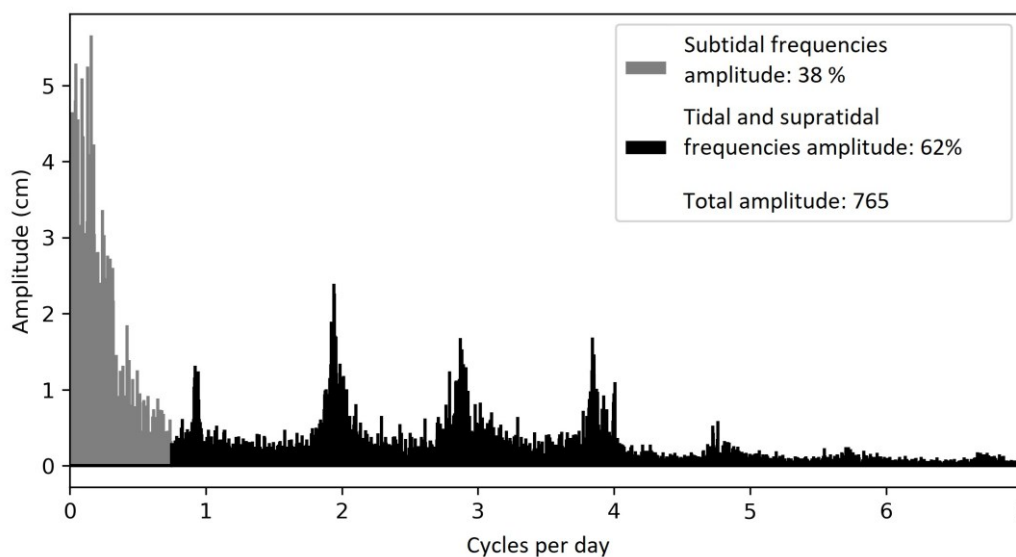
The plot shown in Figure 4 indicates an increase in the amplitude of the M2 wave from the estuary mouth toward the head, suggesting that reflection plays a significant role in enhancing the principal semidiurnal constituents within Paranaguá Bay.

### 3.2.2 RESIDUALS

Residuals are defined as the difference between tide gauge observations and the tidal model generated from the constituents obtained through harmonic analysis. Their magnitude reflects meteorological influences combined with a random component. The application of the model does not always incorporate all relevant frequencies due to limitations of the analysis method, the length of the time series, among other factors. Figure 5 presents the frequency spectrum of the residuals from the CSW\_M series. Peaks in amplitude are observed at tidal and supratidal frequencies over a noise background that decreases with increasing frequency, as expected, since the tide gauge system attenuates higher frequencies. A pronounced increase is nevertheless observed at subtidal frequencies.

Equivalent analyses were performed for the longest available series at each tide gauge station (ATN\_B, CAL\_0, COB\_C, CSW\_B, CSW\_F, CSW\_J, CSW\_K, FLX\_E, GLH\_B, GLH\_G, and GLH\_J). In all cases, a substantial contribution from subtidal components was observed, accounting for between 25% and 52% of the total spectral amplitude. This behavior was identified in both shorter and longer time series, indicating that the amplification of subtidal components is a recurrent characteristic of the analyzed dataset. In addition, a spatial pattern in the contribution of subtidal components was identified. The lowest proportions occurred at the most inner stations of the bay – Antonina (ATN\_B series, 35%) and Ponta do Félix (FLX\_E series, 25%) – whereas the highest subtidal contribution was recorded at Galheta (GLH\_J series, 52%), located at the mouth of the estuarine system.

Figure 5 – Frequency spectrum of the residuals from CSW\_M series.



Source: The authors (2025).

To investigate the behavior of these frequency bands, the data were organized by calendar month, regardless of the year of acquisition. Only months with a minimum of 27 valid observations were considered, in order to ensure statistical representativeness, resulting in a total of 202 groups. Subsequently, the Thompson low-pass filter was applied, yielding two time series for each monthly segment: one comprising subtidal residuals and another comprising tidal and supratidal residuals. For each month, two histograms were then constructed, one for each series. It was consistently observed that the histograms of subtidal residuals exhibited skewness and a shift in the mean, whereas the histograms of tidal and supratidal residuals displayed an approximately symmetric distribution centered around zero.

To quantify these observations, two statistical tests were applied: a test of the mean ( $H_0$ : mean = 0)

and a normality test ( $H_0$ : normal distribution). The null hypothesis of zero mean was rejected in 78% of the cases for subtidal residuals, compared to 0% for tidal and supratidal residuals. In the normality test, the null hypotheses were rejected in 100% of the cases for subtidal residuals and in 56% of the cases for tidal and supratidal residuals. These results indicate that subtidal residuals predominantly reflect long-period variations associated with meteorological processes acting in the region. Accordingly, monthly subtidal residual series were used to investigate the meteorological tide.

For this purpose, time series corresponding to the same calendar month (e.g., all January values from different years) were grouped into a single monthly dataset. Two methods were then applied to each series in order to assess the predominance of positive or negative sea levels and to identify extreme events.

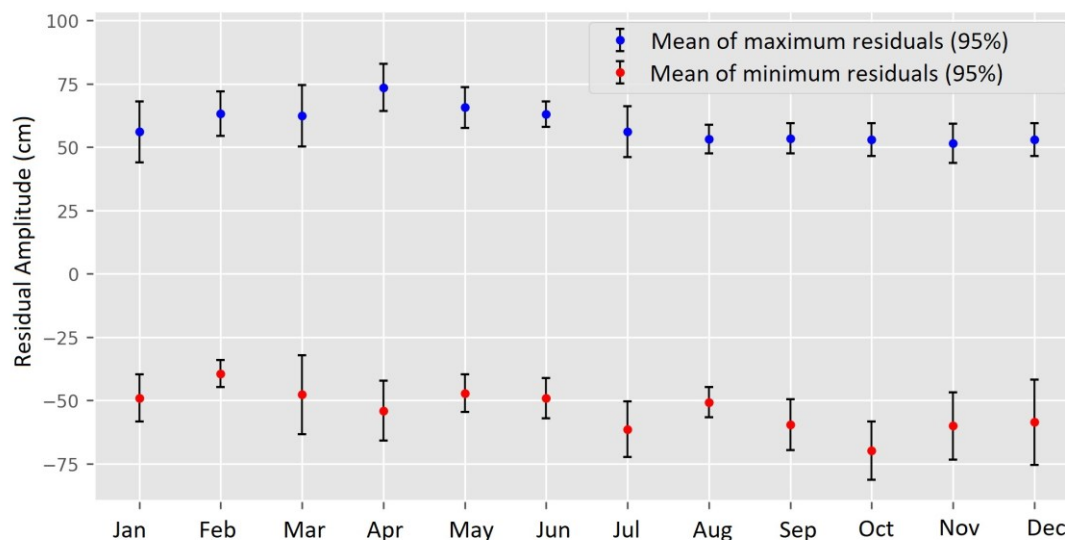
To characterize sea-level predominance, a statistical test was adopted in which the null hypothesis assumes a zero mean. When rejected, the existence of predominance is inferred, being classified as positive when the mean is greater than zero and negative when it is less than zero.

For the identification of extreme events, the normality of the residual distribution was assessed. When normality was rejected, the residuals were ranked and analyzed using percentiles, with negative extremes defined when  $|P5| > |P95|$  and positive extremes otherwise. When the null hypothesis of normality was accepted, the absence of extreme predominance was assumed.

As a result, a predominance of positive sea-level anomalies was observed for the months from February to June, and of negative anomalies for July and November. Positive extreme events predominated from December to July, with higher frequencies in April, May, and June, whereas negative extreme events were more frequent from August to November.

Based on the residuals across all frequency bands (subtidal, tidal, and supratidal), monthly means of maximum and minimum values were calculated with a 95% confidence interval. Figure 6 shows that the largest positive residuals occur during the first half of the year, peaking in April, whereas lower sea levels predominate in the second half of the year, with extreme events concentrated in October. The analysis of subtidal residuals revealed the presence of seasonal patterns associated with the action of meteorological forcings in the region.

Figure 6 – Monthly means of residuals (maxima and minima) with 95% confidence intervals, derived from the set of analyzed series.



Source: The authors (2025).

From the daily mean sea-level data, monthly mean sea levels were computed, and based on these values, the mean monthly sea level throughout the year was estimated. This procedure was applied only to the Cais Oeste and Galheta tide gauges due to the length of the available time series. For clarity, the results are presented in Figure 7, which includes the monthly mean sea levels for Cais Oeste (CSW) and Galheta (GLH), the Sa constituent for both stations, and the monthly sea level at Cananeia, São Paulo.

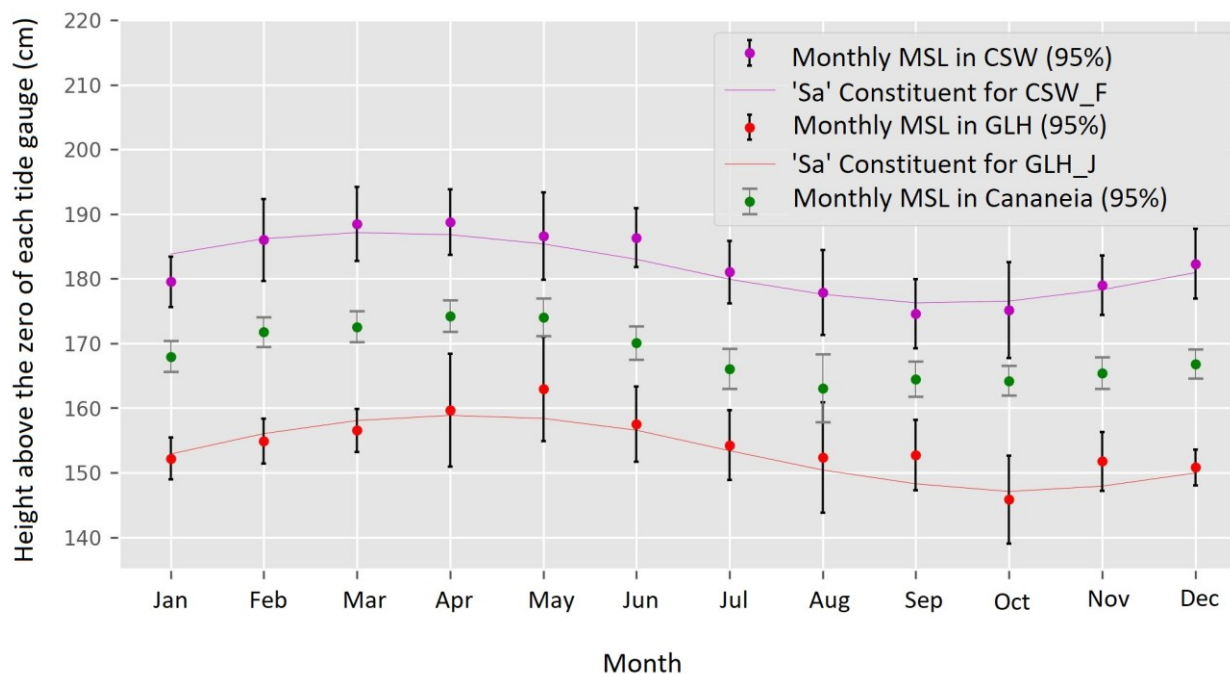
The error bars in the figure represent the 95% confidence interval of the monthly mean sea level,

calculated from the interannual variability of the monthly means. For the GLH and CSW series, which have a smaller number of observations per month, Student's t distribution was applied. For the Cananeia series, which contains a larger number of records, the normal approximation (1.96) was employed, as it is appropriate for large samples.

The Sa constituent corresponds to the annual term of sea-level variability, primarily associated with seasonal oscillations in air temperature and atmospheric pressure, as well as with variations in solar radiation throughout the year. This component allows the identification of seasonal trends in sea-level behavior and supports the interpretation of long-period oscillations.

Analysis of Figure 7 reveals a strong correlation between the annual variability of MSL and the Sa constituent, reinforcing the seasonal nature of sea-level oscillations in the region. This relationship is quantitatively confirmed by the correlation coefficients between monthly MSL and the Sa component, which reach 0.92 for the Cais Oeste station and 0.88 for the Galheta station. Furthermore, the Cananeia tide gauge, located approximately 80 km from Paranaguá, exhibits a similar pattern of variability, with high monthly correlations relative to the Galheta ( $r = 0.90$ ) and Cais Oeste ( $r = 0.95$ ) stations, suggesting a regional influence on these long-period sea-level oscillations.

Figure 7 – Monthly Mean Sea Level for CSW and GLH.



Source: The authors (2025).

#### 4 FINAL CONSIDERATIONS

This study presented a comprehensive analysis of tide gauge data from Paranaguá Bay, Paraná State, with the aim of characterizing regional tidal patterns and associated sea level variability. The analysis was based on tide gauge series obtained from the BNDO, complemented by long-term records from the Cananéia station (SP) provided by the UHSLC.

The adopted methodology followed Intergovernmental Oceanographic Commission (2020) and included the systematic removal of spurious observations. As a key result, an average reduction of 9.86% in the variance of harmonic constituents computed by PACMARÉ was achieved, with particularly pronounced reductions in series ranging from 200 to 400 days in length, notably CSW\_M (62.49% over 309 days) and GLH\_B (53.94% over 215 days). In twelve series, this variance reduction was accompanied by an increase in the number of resolved constituents, indicating enhanced spectral resolution. Variance reductions differed according to tidal frequency bands, amounting to 10.38%, 9.39%, 8.86%, and 10.81% for one, two, three, and four cycles per day, respectively. With respect to data editing, 25 of the 37 series exhibited removal rates below 0.5%, eight series between 0.5% and 1%, and only four series exceeded 1%, with a maximum of

2.02% in series FLX\_D.

Harmonic analysis was performed using both AstGeoTop and PACMARÉ, yielding consistent amplitude estimates and reinforcing the robustness of the applied methods. PACMARÉ resolved a larger number of constituents, particularly shallow-water components, while AstGeoTop proved advantageous for time-domain analysis of series containing data gaps. Semidiurnal tidal behavior was identified at Antonina, Ponta do Félix, and Cais Oeste stations, whereas a semidiurnal regime with inequalities characterized Ilha das Cobras and Galheta.

Spectral analysis of the residuals allowed clear discrimination between tidal, subtidal, and supratidal components, distinguishing random variability from meteorologically driven signals. Subtidal residuals exhibited marked seasonal patterns, with a predominance of positive sea level anomalies between February and June and negative anomalies between July and November. Monthly mean sea level estimates for Cais Oeste and Galheta showed strong correlations with the annual constituent  $S_a$ , with correlation coefficients of 0.92 and 0.88, respectively. Comparable behavior was observed in the Cananéia records, suggesting a regional-scale influence on long-period sea level variability.

Despite these contributions, certain limitations must be acknowledged. The length of the available series is adequate for operational analyses but insufficient for robust long-term assessments of mean sea level trends. Moreover, the absence of complementary meteorological data constrained the identification of atmospheric forcing mechanisms associated with residual variability, as demonstrated in other Brazilian estuarine systems. In Paranaguá Bay, this limitation restricts interpretation to a predominantly mareographic perspective and highlights the need for interdisciplinary approaches in future research.

Finally, this study demonstrates the relevance of harmonic and spectral analyses for understanding residual sea level variability in Paranaguá Bay. The applied methods enabled effective filtering, consistent residual characterization, and the identification of seasonal patterns, providing valuable technical support for applications in coastal engineering, oceanography, cartography, and climatology.

### Authors' Contributions

Author R.S.M.N. carried out the conceptualization, drafted the initial manuscript, and performed revisions and edits. Authors C.P.K. and R.D. supervised the work and conducted the initial reviews..

### Conflicts of interest

The authors have no conflicts of interest to declare.

### References

- Amb Planejamento Ambiental e Biotecnologia Ltda. (2005). Diagnóstico Ambiental [Relatório técnico em PDF]. In: *Estudo de Impacto Ambiental (EIA) do Terminal Portuário localizado no município de Pontal do Paraná, PR* (Cap. 5, pp. 5-1 – 5-215), Universidade Federal do Paraná, Docs UFPR. [https://docs.ufpr.br/~edugeo/Estudos\\_Ambientais\\_Litoral/2005\\_EIA\\_RIMA\\_PortoPontal/EIA/Cap%C3%ADtulo%205/Cap%C3%ADtulo%205.1%20diagn%C3%B3stico%20ambiental%20meio%20fisico.pdf](https://docs.ufpr.br/~edugeo/Estudos_Ambientais_Litoral/2005_EIA_RIMA_PortoPontal/EIA/Cap%C3%ADtulo%205/Cap%C3%ADtulo%205.1%20diagn%C3%B3stico%20ambiental%20meio%20fisico.pdf).
- Andrade, I. O., Carvalho, A. B.; Silva, S. T. & Mont'Alverne, T. C. F. (2024) *Economia azul e crescimento econômico: o mar brasileiro em perspectiva*. Instituto de Pesquisa Econômica e Aplicada. <https://doi.org/10.38116/td3027-port>.
- Boon, J. D. (2007). *Secrets of the Tide*. Woodhead Publishing.
- Caldwell, P. C., Merrifield, M. A. & Thompson, P. R. (2015). *Sea level measured by tide gauges from global oceans as part of the Joint Archive for Sea Level (JASL)*. <https://doi.org/10.7289/v5v40s7w>.
- Camargo, R. & Harari, J. (2003). Modeling the Paranagua Estuarine Complex, Brazil: tidal circulation and cotidal charts. *Revista Brasileira de Oceanografia*, 51, p. 23-31.

- Courtier, A. (1938). Classification of tides in four types. *Conférences sur les Marées*. Service Hydrographique de la Marine Française. <https://journals.lib.unb.ca>
- Dalazoana, R. (2006). *Estudos dirigidos à análise temporal do Datum Vertical Brasileiro*. [Tese de doutorado, Universidade Federal do Paraná]. Acervo Digital da UFPR. <https://acervodigital.ufpr.br>.
- Franco, A. dos S. (2009). *Marés, Fundamentos, Análise e Previsão*. 2a ed. Diretoria de Hidrografia e Navegação.
- Franz, G. A. S., Marone, E., Noernberg, M. A., Zaleski, S., & Lautert, L. F. (2016). From regional to local scale modelling on the south-eastern Brazilian shelf: Case study of Paranaguá estuarine system. *Brazilian Journal of Oceanography*, 64(3), 277–294. <https://www.scielo.br/j/bjoce/a/NHCJ8s9nyYZ9JDFNd6yStmK/?format=pdf>.
- Garnés, S. J. A. (2021). *AstGeoTop Módulo Análise de Maré* [Software, versão 2016]. Universidade Federal de Pernambuco.
- Governo do Estado do Paraná. (2025a). Portos do Paraná bate recorde de movimentação em um único mês: 7,3 milhões de toneladas. <https://www.parana.pr.gov.br/aen/Noticia/Portos-do-Parana-bate-recorde-de-movimentacao-em-um-unico-mes-73-milhoes-de-toneladas>.
- Governo do Estado do Paraná. (2025b). Portos do Paraná bate recorde de movimentação de cargas no primeiro semestre de 2025. <https://www.parana.pr.gov.br/aen/Noticia/Portos-do-Parana-bate-recorde-de-movimentacao-de-cargas-no-1o-semester-de-2025>.
- Governo do Estado do Paraná. (2025c). Com menos restrições de manobras, Porto de Paranaguá ampliará produtividade. <https://www.parana.pr.gov.br/aen/Noticia/Com-menos-restricoes-de-manobras-Porto-de-Paranagua-ampliará-produtividade>.
- Hague, B. S., Jones, D. A., Trewin, B., Jakob, D., Murphy, B. F., Martin, D. J. & Braganza, K. (2022). Anchors: a multi-decadal tide gauge dataset to monitor australian relative sea level changes. *Geoscience Data Journal*, v. 9, p. 256-272. <https://doi.org/10.1002/gdj3.136>.
- Harris, C. R., Millman, K. J., Van der Walt, S. J., Gommers, R., Virtanen, P., Cournapeau, D., Wieser, E., Taylor, J., Berg, S., Smith, N. J., Kern, R., Picus, M., Hoyer, S., van Kerkwijk, M. H., Brett, M., Haldane, A., Fernández del Río, J., Wiebe, M., Peterson, P., & Oliphant, T. E. (2020). Array programming with NumPy. *Nature*, 585(7825), 357–362. <https://doi.org/10.1038/s41586-020-2649-2>.
- Hunter, J. D. (2007). Matplotlib: A 2D graphics environment. *Computing in Science & Engineering*, 9(3), 90–95. <https://doi.org/10.1109/MCSE.2007.55>.
- Intergovernmental Oceanographic Commission. (2020). *Quality control of in situ sea level observations: a review and progress towards automated quality control. (Vol 1)*. UNESCO. <https://unesdoc.unesco.org/ark:/48223/pf0000373566>.
- Kalil, A. F. D. (1999). *Contribuições ao estudo do nível médio do mar no Estado do Rio de Janeiro* [Dissertação de mestrado, Universidade Federal do Rio de Janeiro]. Repositório de dissertações da Engenharia Oceânica da UFRJ. [https://w1files.solucaoatrio.net.br/atrio/ufrij-peno\\_upl//THESIS/10002586/1999\\_mestrado\\_afonse\\_kalil\\_20220125105357605.pdf](https://w1files.solucaoatrio.net.br/atrio/ufrij-peno_upl//THESIS/10002586/1999_mestrado_afonse_kalil_20220125105357605.pdf).
- Marinha do Brasil (2023). *NORMAM-501/DHN*. Diretoria de Hidrografia e Navegação. <https://www.marinha.mil.br/dhn/normas-legislacoes>.
- Marinha do Brasil (2025a). *Carta náutica nº 1820 – Proximidades da Barra de Paranaguá*. Centro de Hidrografia da Marinha. [https://www.marinha.mil.br/chm/dados-do-segnav/cartas-raster?field\\_numero\\_raster\\_value=1820&title=](https://www.marinha.mil.br/chm/dados-do-segnav/cartas-raster?field_numero_raster_value=1820&title=)
- Marinha do Brasil (2025b). *Plano de Levantamento da Plataforma Continental Brasileira (LEPLAC)* Comissão Interministerial para os Recursos do Mar (CIRM). <https://www.marinha.mil.br/secirm/pt-br/leplac>.
- Marone, E., Noernberg, M. A., Lautert, L. F., Santos, I., Fill, H. D., Buba, H., & Marenha, A. (2007). *Medições de correntes e curva vazão-maré na Baía de Paranaguá, PR*. Boletim Paranaense de Geociências, 60. Biblioteca Digital de Periódicos da Universidade Federal do Paraná

<https://doi.org/10.5380/geo.v60i0.9598>.

- Marone, E., Raicich, F., & Mosetti, R. (2013). Harmonic tidal analysis methods on time and frequency domains: similarities and differences for the Gulf of Trieste, Italy, and Paranaguá Bay, Brazil. *Bollettino di Geofisica Teorica ed Applicata*, 54(2), 183–204. [https://bgo.ogs.it/sites/default/files/pdf/bgta0068\\_MARONE.pdf](https://bgo.ogs.it/sites/default/files/pdf/bgta0068_MARONE.pdf).
- Melo Filho, E. (2017). *Maré meteorológica na costa brasileira* [Tese de Professor Titular]. Escola de Engenharia, Universidade Federal do Rio Grande. [https://sistemas.furg.br/sistemas/sab/arquivos/conteudo\\_digital/000008808.pdf](https://sistemas.furg.br/sistemas/sab/arquivos/conteudo_digital/000008808.pdf).
- Moura Neto, J. S., & Azevedo, M. A. L. (2022). *O Brasil e o mar no século XXI: Subsídios para o aproveitamento sustentável do mar brasileiro* (3a ed.). Quiteriense Serviços Gráficos e Editoriais.
- Oliveira, M. M. F. de. (2004). *Redes neurais artificiais na previsão da maré meteorológica em Paranaguá – PR* [Dissertação de Mestrado, Universidade Federal do Rio de Janeiro]. Portal de Dados Abertos da CAPES. [https://www.oasisbr.ibict.br/vufind/Record/BRCRIS\\_66119b586ff4d1b3805869454359b0d7](https://www.oasisbr.ibict.br/vufind/Record/BRCRIS_66119b586ff4d1b3805869454359b0d7)
- Pugh, D. T. (1987). *Tides, Surges and Mean Sea-Level*. John Wiley & Sons. <https://eprints.soton.ac.uk/19157/1/sea-level.pdf>.
- R Core Team. (2022). *R: A Language and Environment for Statistical Computing (Version 4.2.0)* [Computer software]. <https://search.gesis.org/publication/zis-RCoreTeam.2022R>.
- Secretaria de Meio Ambiente, Infraestrutura e Logística (2024). *Sistema inédito antecipa risco de ressacas e desastres naturais na costa paulista*. Governo do Estado São Paulo. <https://semil.sp.gov.br/2024/09/sistema-inedito-antecipa-em-ate-4-dias-risco-de-ressacas-e-desastres-naturais-na-costa-paulista/>.
- Silva, L. M. da, & Freitas, S. R. C. de (2019). Análise da evolução temporal do datum vertical brasileiro de Imbituba. *Revista Cartográfica*, 98, 33–57. [https://www.scielo.org.mx/scielo.php?script=sci\\_arttext&pid=S2663-39812019000100033](https://www.scielo.org.mx/scielo.php?script=sci_arttext&pid=S2663-39812019000100033).
- Sweet, W. V., Dusek, G. P., Obeysekera, J. T. B., & Marra, J. J. (2018). *Patterns and projections of high tide flooding along the U.S. coastline using a common impact threshold* [NOAA Technical Report NOS CO-OPS 086]. Center for Operational Oceanographic Products and Services, National Oceanic and Atmospheric Administration. <https://doi.org/10.7289/V5/TR-NOS-COOPS-086>.
- Tecchio, R., Souza, D. C. de, Silva, M. B. L. da, Costa, M. C. de O., Camargo, R., & Harari, J. (2025). Mean sea level, tidal components and surges in Guanabara Bay (Rio de Janeiro) from 1990 to 2021. *International Journal of Climatology*, 44 (13), 4629-4648. <https://doi.org/10.1002/joc.8600>.
- Virtanen, P., Gommers, R., Oliphant, T. E., Haberland, M., Reddy, T., Cournapeau, D., Burovski, E., Peterson, P., Weckesser, W., Bright, J., Walt, S. J. van der, Brett, M., Wilson, J., Millman, K. J., Mayorov, N., Nelson, A. R. J., Jones, E. Kern, R., Larson, E., ... & Vanderplas, J. (2020). SciPy 1.0: Fundamental algorithms for scientific computing in Python. *Nature Methods*, 17, 261–272. <https://www.nature.com/articles/s41592-019-0686-2>.

## Biography of the main author



Raimundo Sales de Melo Neto was born in Rio de Janeiro, Brazil. He is a Cartographic Engineer from the State University of Rio de Janeiro in 2007. He has experience in topography and cartography applied to the design and execution of civil engineering projects. He currently serves in the Brazilian Navy at the Hydrographic Center (CHM), contributing to the production of nautical charts.



Esta obra está licenciada com uma Licença [Creative Commons Atribuição 4.0 Internacional](https://creativecommons.org/licenses/by/4.0/) – CC BY. Esta licença permite que outros distribuam, remixem, adaptem e criem a partir do seu trabalho, mesmo para fins comerciais, desde que lhe atribuam o devido crédito pela criação original.